Hindawi Publishing Corporation
Advances in Meteorology
Volume 2015, Article ID 585623, 9 pages
http://dx.doi.org/10.1155/2015/585623

Research Article

Influence of Urban Microclimate on Air-Conditioning Energy Needs and Indoor Thermal Comfort in Houses

Feng-Chi Liao,[1] Ming-Jen Cheng,[2] and Ruey-Lung Hwang[3]

[1]*Ph.D. Program in Civil and Hydraulic Engineering, Feng Chia University, 100 Wenhwa Road, Taichung 407, Taiwan*
[2]*Department of Architecture, Feng Chia University, 100 Wenhwa Road, Taichung 407, Taiwan*
[3]*Department of Architecture, National United University, 1 Lienda, Miaoli 360, Taiwan*

Correspondence should be addressed to Ruey-Lung Hwang; rueylung@nuu.edu.tw

Received 24 September 2014; Revised 19 March 2015; Accepted 24 March 2015

Academic Editor: Panagiotis Nastos

A long-term climate measurement was implemented in the third largest city of Taiwan, for the check of accuracy of morphing approach on generating the hourly data of urban local climate. Based on observed and morphed meteorological data, building energy simulation software EnergyPlus was used to simulate the cooling energy consumption of an air-conditioned typical flat and the thermal comfort level of a naturally ventilated typical flat. The simulated results were used to quantitatively discuss the effect of urban microclimate on the energy consumption as well as thermal comfort of residential buildings. The findings of this study can serve as a reference for city planning and energy management divisions to study urban sustainability strategies in the future.

1. Introduction

Approximately 70% of Taiwan's population lives in cities. With the expansion of the urban scale, the urban heat island (UHI) effect has become increasingly significant. Lin et al. [1] indicated that UHI is common to cities of Taiwan, especially metropolises. The population/area of the three major cities of Taiwan, namely, Taipei, Kaohsiung, and Taichung, is, respectively, 2.6 million/272 km^2, 1.5 million/154 km^2, and 1.2 million/163 km^2. They are also the top three cities in the UHI intensity, which is 4.5°C, 3.2°C, and 2.7°C, respectively. Increasingly UHI effect and global warming accelerate the deterioration of urban microclimate, thereby influencing the urban livability significantly. Architects are thus confronted with more austere challenges in architectural design.

Urban microclimate change directly influences building energy consumption and indoor thermal comfort; this has become a topical subject in many countries. Kolokotroni et al. [2] found that the UHI effect is an important factor in the underestimation of urban building energy consumption. Taking Britain as an example, the rural office building energy consumption for cooling is only 84% of urban consumption. Jusuf et al. [3] simulated the differences in the energy consumption of office buildings in various large cities of the USA under the UHI effect. The results showed that the urban ambient temperature, due to the UHI effect, was higher than the suburban temperature by 2°C on average. The energy consumption for cooling buildings was increased by 17.25%, and energy consumption for heating was reduced by 17.04%. Sun and Augenbroe [4] found that the cooling degree hours of 15 big cities of the USA were greater than that of rural districts by 25.3% on average due to the UHI effect. In Australia, Ren et al. [5] conducted thermal performance simulation for the buildings in urban, rural, and urban-green regions. The results showed that a green area could reduce the downtown maximum ambient temperature by 0.8°C, which changed the heat stress risk level of buildings from "severe" to "moderate." Oxizidis et al. [6] reported that in Lisbon, due to the UHI effect, the energy consumption for heating of buildings in the city center was lower than that in the suburbs. Wong et al. [7] found that different block designs in Singapore influence the urban ambient temperature by 0.9–1.2°C. Therefore, if urban blocks are planned properly, the energy consumption for cooling of buildings can be reduced by 5–10%. Wong et al. [8] indicated that microclimate change in a campus could change the building energy consumption by 2.3–14.3%. Chan

[9] indicated that the energy consumption for cooling urban buildings in Hong Kong was higher than that of suburban buildings by about 10%.

The goal of building designers is to create an energy-saving and comfortable residential environment. Therefore, it is necessary and urgent to explore the influence of urban microclimate on building energy consumption and indoor thermal environments and collect a set of highly reliable urban local climate data. To our best knowledge, there is no related research in Taiwan. In view of this, this study collects the microclimate data of different locations in the city by long-term field measurement and the morphing approach and used EnergyPlus [10] to simulate energy consumption for cooling and indoor thermal comfort of residential construction. The quantified data on the effect of the variance of Taiwan's urban microclimate on building energy consumption and indoor environment quality can serve as reference data for city planning and energy management divisions to study urban sustainability strategies in the future.

2. Methodology

2.1. Morphing Approach. Current building thermal performance is evaluated based on the hourly meteorological data of weather stations by simulation software, such as EnergyPlus, in order to simulate the energy consumption of buildings. However, as the weather stations are located in the suburbs and each city usually has only one weather station, it is difficult to obtain the hourly microclimate data of any site in the city. Therefore, studies [5, 7–9], which analyzed the effect of urban microclimate change on energy consumption, used field measurements and the morphing approach [11] to create the hourly data of urban microclimate. This approach uses the weather station data as the baseline climate and uses the measured data of urban climates to correct the climatic contrasts by shift and linear stretch. Finally, the hourly meteorological data of various places of a city are created. The equations of morphing approach are as follows:

$$\begin{aligned} T &= T_0 + \Delta T_m + \alpha T_m \left(T_0 - T_m\right), \\ \alpha T_m &= \frac{\Delta T_{\max,m} - \Delta T_{\min,m}}{T_{\max,m} - T_{\min,m}}, \\ s &= s_0 \times \alpha s_m, \\ \alpha s_m &= 1 + \frac{\mathrm{SPHU}_m}{100}, \end{aligned} \tag{1}$$

where T_0 is the hourly ambient temperature from the weather station; T_m, $T_{\max,m}$, and $T_{\min,m}$ are the monthly mean values of ambient temperature, daily maximum temperature, and daily minimum temperature, respectively, for month m; ΔT_m, $\Delta T_{\max,m}$, and $\Delta T_{\min,m}$ are the variations between weather station and urban areas in the monthly mean of ambient temperature, daily maximum temperature, and daily minimum temperature, respectively, for month m; s and s_0 are the hourly specific humidity in urban areas and from weather station; SPHU_m is the change in monthly mean specific humidity given as a percentage for month m; αT_m and αs_m are the fractional change in monthly mean temperature change and monthly mean differences of specific humidity, respectively, for month m.

2.2. Field Measurement. Taichung, the third largest city of Taiwan, was chosen for investigation in this study, because the increase of its annual mean ambient temperature is higher than the other cities of Taiwan, which is +0.40°C/10 years in the past 30 years [12]. Taichung is located in central Taiwan (24°15′N; 120°40′E), and its population is about 1.2 million. The development in the city is centered on the area around the main train station and expands to the new districts. The older buildings are mostly 5 stories or below; the buildings in new districts are mostly 6 to 15 stories. The buildings of 16 stories or above are concentrated along the main road going through the new district.

In terms of climate, Taichung is located in hot-humid climate zone, where the mean annual temperature is 23.3°C in the recent three decades. The maximum monthly mean temperature occurs in July, and the monthly mean temperature in July in the most recent 30 years is 28.6°C. The UHI effect intensity is about 2.7°C in summer.

According to (1), in order to use the morphing approach to create the hourly data of urban microclimate, the monthly mean of hourly temperature, daily maximum temperature, daily minimum temperature, and monthly average specific humidity of the local climate should be known beforehand. Figure 1 shows the positions of the 10 selected sites in the city, as well as a brief description of peripheral environments, including building density and the underlying surface of bared ground, roads, and green area. Two principals applied to select the sites for field measurement are as follows.

(i) All of the selected sites uniformly are distributed from the downtown to suburban areas of the city approximately.

(ii) The selected sites are expected to have different levels of UHI intensity.

The field measurements were collected from July to September 2013. The calibrated ESCORT iLog [13] temperature/humidity data logger was used to measure the air temperature and relative humidity (RH) at each selected site. The data loggers were attached to the electricity posts or lampposts in selected sites, as shown in Figure 2, and configured at 5-minute interval throughout the measurement periods. The air temperature/RH data were obtained by sampling at a height of 3.0 m for each of the selected sites. As a reference, meteorological data were gathered from nearby weather stations, which had been located in a metropolitan park with a large area of water bodies and vegetation. The weather station is maintained by the Central Weather Bureau of Taiwan.

2.3. Building Model. In order to analyze the impact of the UHI effect on building energy consumption and indoor thermal comfort level, this study chose a typical flat as the building model. This was done purposely as there are a wide variety of apartment styles in the country. However, the

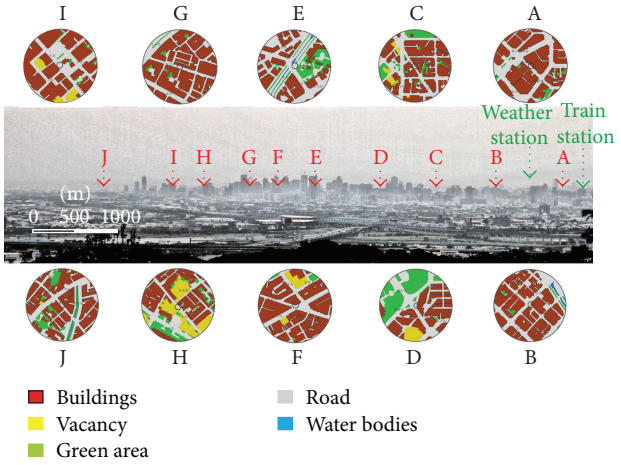

Figure 1: Position and underlying surface type of selected sites for field measurement.

Figure 2: Installation of temperature/humidity data logger at a selected site.

energy simulation of typical buildings under representative operation conditions may contribute to a better understanding on the average energy performance of buildings in Taiwan. The analysis can serve as a preliminary comparison of the impact of UHI.

The residential apartment is a 3-bedroom residential flat of area 90 m^2 with a rectangular living/dining room. The prevailing summer wind in Taiwan is south wind; thus the windows of flat are arranged on the south and north façade for natural ventilation. The south wall has an overhang, and the south windows are shaded by the attached overhang. Other pieces of information for the construction of walls/windows, internal gains, and air conditioner used in this typical flat are listed in Table 1.

2.4. Calculation of Energy Consumption for Cooling and Thermal Comfort. The typical flat was simulated in air-conditioned and naturally ventilated scenarios (Figure 3).

Table 1: Specifications of construction and air-conditioning system in a typical residential flat.

Item	Description
External wall construction	5 mm mosaic tile (outer layer) 10 mm cement 150 mm heavy concrete 10 mm cement (inner layer)
Glass type	6 mm single clear glass
Gross floor area	90 m^2/flat
Equipment power intensity	140 W/room
Lighting power intensity	8 W/m^2
Indoor design temperature	28°C
Occupancy intensity	4 persons/flat
Operating hours of air conditioner	7:00 pm to 11:00 pm (living room) 8:00 pm to 8:00 am (bedroom)
C.O.P.	3.0

Building simulation software EnergyPlus was used to calculate the cooling energy consumption of air-conditioned typical flat as well as the indoor thermal conditions of naturally ventilated typical flat.

The inclusion of adaptive thermal comfort model in the ASHRAE Standard 55 [14] and EN 15251 [15] exemplifies the increasing effort of improving indoor environmental quality in naturally ventilated or hybrid ventilated buildings. Based on the report by Hwang et al. [16], when the upper limit of the comfort zones projected by these models was compared, the predictability of the ASHRAE model appeared to be less than that of the EN model in the warm condition like Taiwan. The EN comfort zones of Categories I and II were more consistent with field observations than the ASHRAE comfort zones 90 and 80%. Hence, the EN adaptive comfort model was to evaluate the indoor thermal comfort of the typical flat in this study.

As the comfort temperature is influenced by people's clothing, behavior, and level of adaptation, thus the EN adaptive approach considers the comfort temperature to be related to a person's thermal history with more recent experiences being more influential. This makes the exponential weighting attractive as a weight for past temperatures [17]. The exponential weighting system results in decay in the importance of any past temperature. Based on a weekly running average outside air temperature (T_{rm}), the EN adaptive comfort model recommended the upper boundaries of thermal comfort zones for Category II, which is suitable for residential spaces, as given in

$$T_c = 0.33 \times T_{rm} + 21.8 \quad \text{for } 25 \le T_c \le 32^\circ\text{C},$$
$$T_{rm} = \left(T_{-1} + 0.8 \times T_{-2} + 0.6 \times T_{-3} + 0.5 \times T_{-4} + 0.4 \times T_{-5} + 0.3 \times T_{-6} + 0.2 \times T_{-7}\right) \cdot (3.8)^{-1}, \tag{2}$$

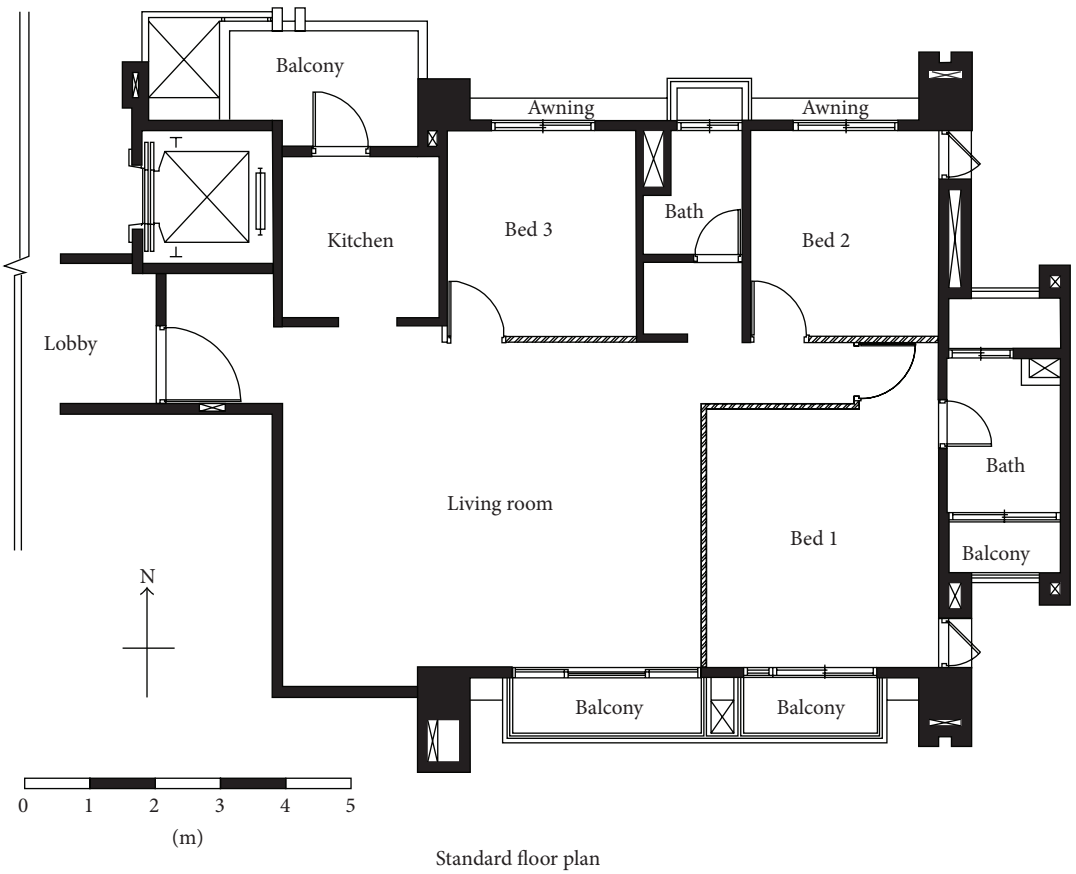

Figure 3: Plan view of the typical flat used in the study.

where T_{-1} is the mean outside air temperature of the previous day, T_{-2} is the mean outside air temperature two days ago, and so forth.

For long-term indoor thermal environment comfort evaluation, ISO 7730 [18] recommends the following two methods:

(i) hours of exceedance (H_e): calculate the number of hours that the building is occupied, and the operative temperature (t_{op}) is outside a specified range ($t_{o,limit}$);

(ii) weighted exceedance (W_e): the time during which the actual operative temperature exceeds the specified range during the occupied hours is weighted with a factor which is a function of how many degrees the range has been exceeded. The weighting factor (wf) must equal 1 for $t_{op} = t_{o,limit}$. The weighting factor is calculated as follows:

$$wf = 1 + \frac{\left|t_{op} - t_{op,limit}\right|}{\left|t_{op,optimal} - t_{op,limit}\right|}. \quad (3)$$

For a characteristic warm period during a year, the product of the weighting factor, wf, and time t is summed and the result expressed in hours:

$$\sum wf \cdot t \quad \text{for } t_{op} > t_{op,limit}. \quad (4)$$

3. Result of Field Measurement

Figure 4 shows the variation of daily mean temperatures, as measured at the 10 selected sites and from the weather stations during the experimental period. In the four months of the experiment, the daily mean temperature from the weather station was in the range of 25°C–31.6°C. Site D that contained a large area of vegetation had the minimum mean temperature among the 10 selected sites. Site F, surrounded by intensive high-rise buildings and extensive heat discharge from vehicles, had the maximum mean temperature. The mean temperatures measured at various measuring sites were higher than the mean temperature measured at the weather station, and the temperature difference was 1.3°C–2.1°C. In addition, the mean temperature, the maximum daily mean temperature, and minimum daily mean temperature at the 10 selected sites were higher than those from the weather station. Figure 5 shows the daily mean RH from the weather station and selected sites during the experimental period. In the experimental period, the maximum difference of mean RH between selected site and weather station occurred at site G, and the difference was 6%. The values of T_m, $T_{max,m}$, $T_{min,m}$, ΔT_m, $\Delta T_{max,m}$, $\Delta T_{min,m}$, and RH_m of the selected sites and weather station from July to October are as listed in Table 2.

Table 2: Summary of T_m, $T_{\max,m}$, $T_{\min,m}$, ΔT_m, $\Delta T_{\max,m}$, $\Delta T_{\min,m}$ (°C), and RH_m (%) for selected sites.

Month	Climatic variables	Selected sites									
		A	B	C	D	E	F	G	H	I	J
Jul.	T_m	29.7	30.2	29.7	29.4	29.9	30.2	29.9	29.3	29.7	29.7
	$T_{\max,m}$	34.9	35.5	34.8	34.2	35.5	35.6	35.1	34.5	35.3	34.8
	$T_{\min,m}$	26.3	26.7	26.2	26.1	26.0	26.5	26.4	25.8	26.1	26.2
	RH_m	72	71	72	72	72	74	71	74	78	73
	ΔT_m	1.6	2.0	1.6	1.3	1.7	2.1	1.8	1.2	1.5	1.6
	$\Delta T_{\max,m}$	3.0	3.6	2.9	2.3	3.6	3.7	3.2	2.6	3.4	2.9
	$\Delta T_{\min,m}$	1.1	1.5	1.0	0.9	0.7	1.3	1.2	0.6	0.9	1.0
Aug.	T_m	29.7	30.2	29.7	29.4	29.9	30.2	29.9	29.3	29.7	29.7
	$T_{\max,m}$	35.4	35.9	35.3	34.8	36.0	36.1	35.6	35.3	35.7	35.3
	$T_{\min,m}$	27.4	27.7	27.3	27.1	26.9	27.5	27.5	26.9	27.2	27.3
	RH_m	68	67	68	69	69	71	67	70	75	69
	ΔT_m	1.6	2.1	1.6	1.3	1.8	2.2	1.9	1.3	1.6	1.8
	$\Delta T_{\max,m}$	2.9	3.4	2.8	2.4	3.5	3.6	3.1	2.8	3.2	2.8
	$\Delta T_{\min,m}$	1.4	1.8	1.4	1.2	1.0	1.6	1.6	1.0	1.3	1.4
Sep.	T_m	29.2	29.7	29.3	29.0	29.3	29.8	29.5	29.1	29.2	29.3
	$T_{\max,m}$	34.0	34.6	34.0	33.4	34.4	34.7	34.1	34.1	34.1	33.8
	$T_{\min,m}$	26.3	26.7	26.3	26.1	25.9	26.5	26.5	26.0	26.2	26.3
	RH_m	75	73	74	75	76	77	73	76	82	75
	ΔT_m	1.5	2.1	1.6	1.3	1.7	2.2	1.9	1.4	1.5	1.7
	$\Delta T_{\max,m}$	2.8	3.4	2.8	2.2	3.2	3.5	3.0	2.9	3.0	2.6
	$\Delta T_{\min,m}$	1.4	1.8	1.4	1.2	1.0	1.6	1.6	1.0	1.2	1.4
Oct.	T_m	28.3	28.8	28.4	28.0	28.5	28.9	28.6	28.1	28.3	28.4
	$T_{\max,m}$	33.9	34.5	33.8	33.3	34.0	34.4	33.9	33.8	34.1	33.7
	$T_{\min,m}$	25.0	25.4	25.0	24.8	24.7	25.2	25.2	24.6	24.9	25.0
	RH_m	69	68	69	70	70	72	68	71	76	70
	ΔT_m	1.5	2.0	1.5	1.2	1.7	2.1	1.8	1.3	1.5	1.6
	$\Delta T_{\max,m}$	3.0	3.6	3.0	2.4	3.2	3.6	3.1	2.9	3.2	2.8
	$\Delta T_{\min,m}$	1.2	1.5	1.1	1.0	0.9	1.3	1.3	0.8	1.1	1.1

Table 3: Values of αT_m and αs_m, for the morphing approach.

Item	Month	Selected sites									
		A	B	C	D	E	F	G	H	I	J
αT_m	Jul.	0.28	0.31	0.28	0.22	0.43	0.37	0.30	0.30	0.38	0.29
	Aug.	0.22	0.25	0.22	0.18	0.39	0.31	0.23	0.28	0.30	0.22
	Sep.	0.23	0.26	0.23	0.17	0.36	0.31	0.22	0.30	0.28	0.20
	Oct.	0.26	0.29	0.26	0.20	0.32	0.32	0.24	0.31	0.31	0.24
αs_m	Jul.	1.00	1.01	0.99	0.99	1.01	1.07	0.99	1.00	1.07	1.01
	Aug.	0.98	1.00	0.99	0.98	1.01	1.06	0.99	1.00	1.09	1.01
	Sep.	1.01	1.02	1.01	1.01	1.04	1.09	1.01	1.02	1.11	1.02
	Oct.	0.99	1.00	0.98	0.98	1.01	1.06	0.98	1.00	1.09	1.00

4. Accuracy of Morphing Approach

4.1. Comparison of Climatic Data. Table 3 lists the calculated αT_m and αs_m for each selected site. By using the morphing approach, the calculated αT_m, αs_m, T_m, $T_{\max,m}$, $T_{\min,m}$, ΔT_m, $\Delta T_{\max,m}$, $\Delta T_{\min,m}$, and RH_m were used to generate the hourly meteorological data for each selected site. Taking site A as an example, Figure 6 compares the observed temperature and forecasted temperature obtained from the morphing approach in the experiment period. Figure 7 shows the comparison of relative humidity. In addition, the mean absolute bias error (MABE), the index of agreement (IA), and the coefficient of determination R^2 for each selected site were calculated and listed in Table 4. As shown in Table 4, R^2 is >0.88, MABE is <0.98°C, and IA is >0.97 for temperature prediction, and R^2 is >0.85, MABE is <2.38%, and IA is >0.96

Table 4: The R^2, MABE, and IA of $y = ax + b$ for selected sites.

Item	Selected sites									
	A	B	C	D	E	F	G	H	I	J
Temp.										
a	1.02	1.03	1.01	1.01	0.97	0.99	1.00	1.00	1.01	1.03
b	0.60	0.80	0.24	0.26	0.86	0.34	0.13	0.08	0.29	0.92
R^2	0.95	0.95	0.95	0.95	0.88	0.93	0.94	0.93	0.92	0.94
MABE	0.56	0.56	0.54	0.51	0.98	0.75	0.63	0.67	0.76	0.60
IA	0.99	0.99	0.99	0.99	0.97	0.98	0.98	0.98	0.98	0.98
RH										
a	0.85	0.88	0.84	0.84	0.87	0.85	0.82	0.84	0.84	0.85
b	11.5	9.3	11.6	11.9	9.9	11.8	13.5	12.5	12.5	11.5
R^2	0.94	0.93	0.93	0.93	0.87	0.89	0.90	0.90	0.85	0.91
MABE	2.88	2.87	2.98	2.83	3.99	3.85	3.54	3.55	4.39	3.02
IA	0.98	0.98	0.98	0.98	0.96	0.97	0.97	0.97	0.96	0.97

Table 5: Energy consumption for cooling based on observed and morphed weather data.

Energy consumption	Selected sites									
	A	B	C	D	E	F	G	H	I	J
Observed	19.5	20.9	19.6	18.8	20.2	21.8	20.2	19.1	20.6	19.9
Morphed	19.7	21.1	19.8	19.0	20.4	22.0	20.4	19.2	20.7	20.0
Error	1.03	0.96	1.02	1.06	0.99	0.92	0.99	0.52	0.49	0.50

Unit: energy consumption in kWh/m^2; error in %.

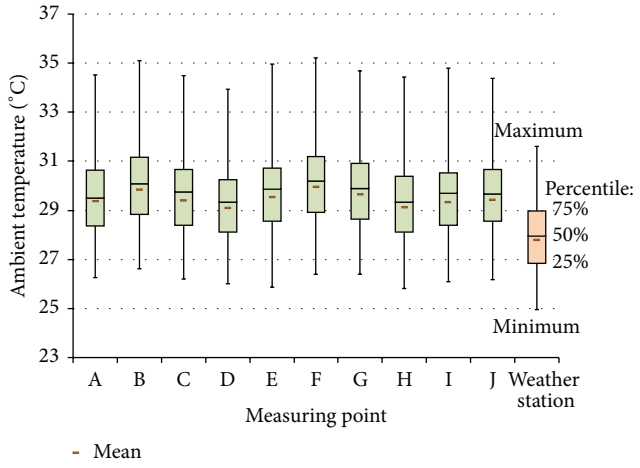

Figure 4: Variation of daily mean ambient temperature of all selected sites as well as the weather station during July to October 2013.

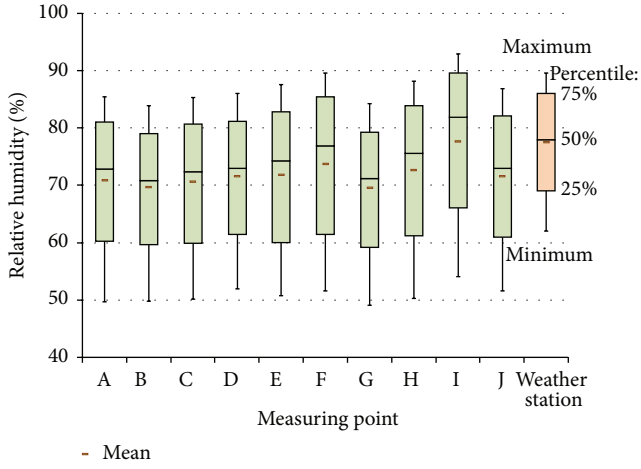

Figure 5: Variation of daily mean RH of all selected sites as well as the weather station during July to October 2013.

for RH prediction. Therefore, it seems reasonable to make a conclusion that the morph approach could be used to forecast urban microclimate.

4.2. Comparison of Energy Consumption for Cooling. In order to determine the effect of the error of the morphing approach in temperature forecasting on the air-conditioning energy consumption and indoor thermal comfort of buildings, the observed meteorological data and morphed meteorological data from the morphing approach were simultaneously used as the input meteorological data for EnergyPlus simulation.

Table 5 summarizes the EnergyPlus simulation results of cooling energy consumption of typical flat in selected sites. As shown in Table 5, the cooling energy consumption for the selected sites, based on observed meteorological data, falls in the range of 21.8–18.8 kWh/m^2, with an average of 20.1 kWh/m^2. Meanwhile, the cooling energy consumption for the selected sites, based on morphed meteorological data, is in the range of 22.0–19.0 kWh/m^2, and the average is

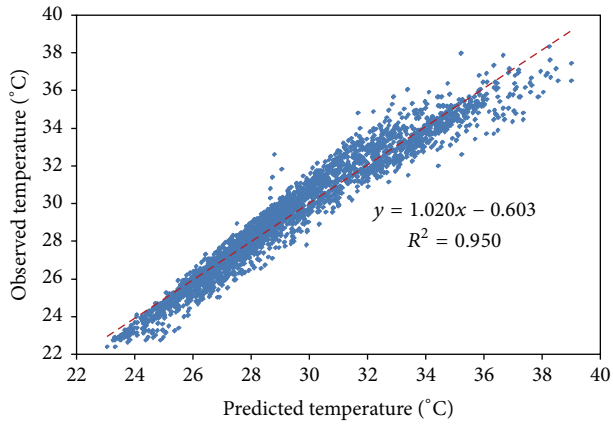

Figure 6: Comparison between measured and morphed hourly temperature at site A.

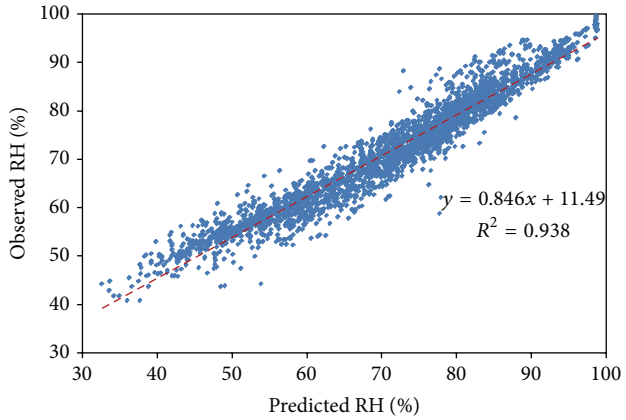

Figure 7: Comparison between observed and morphed hourly RH at site A.

20.2 kWh/m^2. Table 5 also lists the errors, resulting from the usage of different meteorological data source, of the cooling energy consumption at each selected site. As shown in Table 5, the percentage error is only 0.58%–0.83%, which is very low.

4.3. Comparison of Thermal Comfort. Table 6 shows the simulated results of indoor thermal conditions in the naturally ventilated typical flat, based on observed and morphed meteorological data, respectively. Table 6 shows that the H_e and W_e based on morphed meteorological data are higher than the values based on observed meteorological data, with percentage errors for H_e and W_e of 0.7%–17.0% and 5.3%–24.5%, respectively, with an average of 8.8% and 14.2%, respectively, for living room, and for the master bedroom the percentage error of H_e is 8.8%–63.3% with average of 32.8% and the percentage error of W_e is 13.1%–73.0% with an average of 38.5%.

According to the error analysis mentioned above, the urban microclimate data generated from the morphing approach resulted in a slight error on the cooling energy consumption of an air-conditioned typical flat; however, there

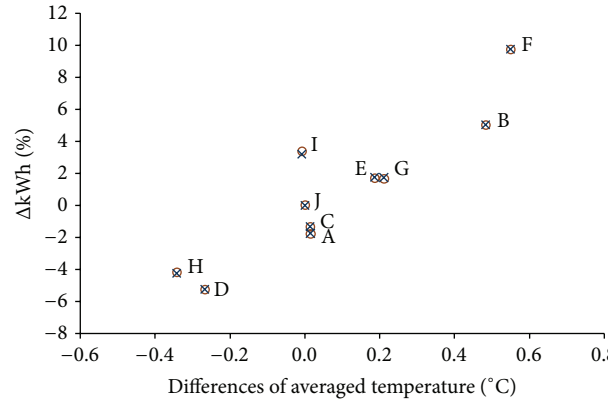

Figure 8: The percentage of ΔkWh versus difference of averaged temperature during July to October 2013.

was a moderate large error in the indoor thermal comfort level of a naturally ventilated typical flat. In other words, the hourly urban microclimate data generated by morphing methodology were probably only applicable to forecasting the energy consumption of air-conditioned houses. If morphing methodological data were used for analyzing the indoor thermal comfort level of naturally ventilated spaces, additional attention should be paid because of the moderate errors they did.

5. Impact of Urban Microclimate

Figure 8 shows the scatter plot of the percentage, compared to the baseline site, of cooling energy consumption change (ΔkWh) against the differences, between baseline site and remainder sites, of mean ambient temperature in the experiment period. Since Lin et al. [1] used the temperature in urban fringe as baseline temperature to determine the UHI intensity of Taichung, site J, which locates in the urban fringe, rather than the weather station, was selected as baseline site. This is helpful for the linkage of the findings between previous study and this study.

The data showed that the cooling energy consumption at the site F, which has the hottest urban microclimate during the experiment period, is higher by 10% than that at baseline site J. For site D with a large green area to relieve its microclimate, the energy consumption for cooling is lower than that at baseline site J by 5%. According to the simulated results, a 1°C of increase in averaged ambient temperature in urban areas during the experiment period would lead to an increase of cooling energy consumption by 14.2%, when compared to that in the suburbs.

The H_e and W_e of site J are used as the baseline values, and the differences between H_e and W_e of the living room and master bedroom at baseline site and remainder sites (i.e., ΔH_e and ΔW_e) are calculated, in order to learn the effect of the variance in urban microclimate on the indoor thermal comfort of a naturally ventilated house.

Figure 9 shows the percentage of H_e change (ΔH_e), and the percentage of W_e change (ΔW_e) is shown in Figure 10. At

Table 6: H_e and W_e for naturally ventilated living room and bedroom at each site.

Item	Weather data	Selected sites									
		A	B	C	D	E	F	G	H	I	J
		Living room									
H_e	Obser.	391	516	408	326	381	526	464	311	360	432
	Morph.	420	536	428	365	439	546	497	364	416	435
	Error	7.4	3.9	4.9	12.0	15.2	3.8	7.1	17.0	15.6	0.7
W_e	Obser.	485	684	512	400	474	698	595	374	447	546
	Morph.	548	738	562	460	591	765	667	462	545	575
	Error	12.9	7.8	9.7	15.0	24.5	9.6	12.2	23.3	21.8	5.3
		Master bedroom									
H_e	Obser.	357	625	374	257	311	596	491	205	305	445
	Morph.	460	680	480	341	508	720	588	334	451	508
	Error	28.9	8.8	28.3	32.7	63.3	20.8	19.8	62.9	47.9	14.2
W_e	Obser.	417	764	437	296	365	727	582	234	355	524
	Morph.	556	864	582	403	631	927	733	400	548	617
	Error	33.4	13.1	33.2	36.3	73.0	27.4	26.0	70.5	54.4	17.6

Unit: H_e in hour; W_e in °C-hour; error in %.

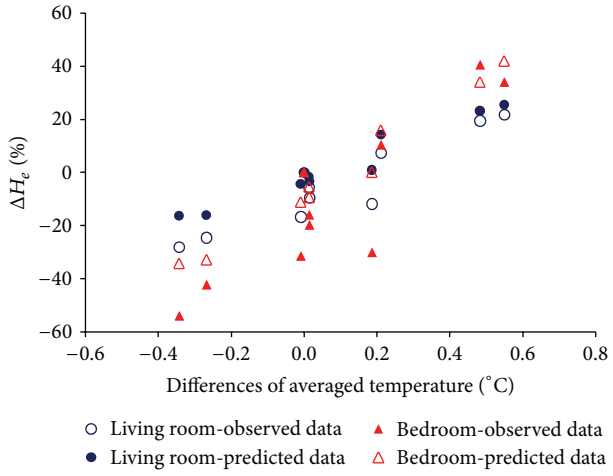

Figure 9: The percentage of ΔH_e versus difference of averaged temperature during investigated period.

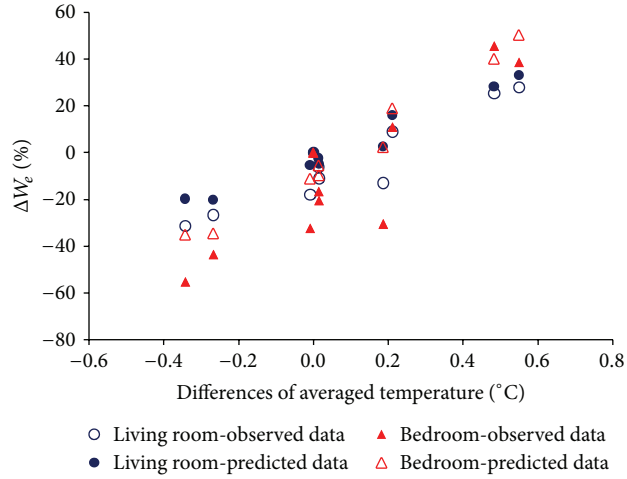

Figure 10: The percentage of ΔW_e versus difference of averaged temperature during the research period.

the hottest site F, the overheating hours of the living room and master bedroom are longer, by 22% and 34%, respectively, than baseline site J. At the coolest site D, the overheating hours are shorter by 25% and 42% for living room and master bedroom, respectively. As compared to the simulated data in suburban, if the mean outside air temperature in the urban was increased by 1°C, the hours of exceedance for the naturally ventilated living room and bedroom would be increased by 56% and 100%, respectively.

Regarding the effect of UHI on W_e, as compared with the result of baseline site J, when the difference of averaged temperature increases from the minimum −0.34°C to the maximum 0.55°C, the percentage of W_e of the living room increases from −27% to 28%, while that of the master bedroom increases from −44% to 39%. If the mean outside air temperature in urban increases by 1°C, the weighted exceedance of naturally ventilated living room and bedroom would be increased by 66% and 108%, respectively. Figures 9 and 10 also show the results based on predicted weather data for comparison.

6. Conclusion

This study quantitatively discussed the effect of UHI on building energy consumption for cooling and indoor thermal comfort by long-term field measurements and EnergyPlus simulation. Moreover, it verified the accuracy of the morphing approach in generating urban microclimate data. The important findings are as follows.

Three statistical indices, including R^2, MABE, and IA, were used to observe the accuracy of morphing approach in forecasting the urban microclimate data. The result showed

that the morphing approach has good accuracy in forecasting temperature and RH. In terms of the error of cooling energy consumption, the percentage error of the observed and predicted meteorological data is slight with a range of 0.49%–1.06%. However, the meteorological data generated from the morphing approach made moderate errors in the assessment of thermal comfort in a naturally ventilated space. This suggests that the climatic data generated from morphing approach are suitable for the analysis of energy consumption of air-conditioned buildings but not suitable for the diagnosis of indoor thermal comfort level of naturally ventilated buildings.

Moreover, the cooling energy consumption, hours of exceedance, and weighted exceedance are positively correlated with the mean outside air temperature. With the suburban selected site as the baseline, an increase of mean ambient temperature by 1°C during the experiment period (July to October) will make an increment of 14.2% in cooling energy consumption in an air-conditioned typical flat. The hours of exceedance of the living room and master bedroom of a naturally ventilated typical flat are increased by 56% and 100%, respectively. The weighted exceedance is increased by 66% and 108%, respectively. The findings of this study can serve as a reference for city planning and energy management divisions to study urban sustainability strategies in the future.

Disclaimer

The funding source was not involved in the study design, the collection, analysis, and interpretation of data, the writing of report, or the decision to submit the paper for publication.

Conflict of Interests

The authors declare that there is no conflict of interests regarding the publication of this paper.

Acknowledgment

The authors offer their sincere appreciation for assistance in grant to the Ministry of Science and Technology, Taiwan, under Project no. NSC-103-2221-E-239-020.

References

[1] H. T. Lin, K. P. Lee, K. T. Chen, L. J. Lin, H. C. Kuo, and T. C. Chen, "Experimental analyses of urban heat island effects of the four metropolitan cities in Taiwan (I)—the comparison of the heat island intensities between Taiwan and the world cities," *The Journal of Architecture*, vol. 31, pp. 51–73, 1999.

[2] M. Kolokotroni, I. Giannitsaris, and R. Watkins, "The effect of the London urban heat island on building summer cooling demand and night ventilation strategies," *Solar Energy*, vol. 80, no. 4, pp. 383–392, 2006.

[3] S. K. Jusuf, N. H. Wong, E. Hagen, R. Anggoro, and Y. Hong, "The influence of land use on the urban heat island in Singapore," *Habitat International*, vol. 31, no. 2, pp. 232–242, 2007.

[4] Y. Sun and G. Augenbroe, "Urban heat island effect on energy application studies of office buildings," *Energy and Buildings*, vol. 77, pp. 171–179, 2014.

[5] Z. Ren, X. Wang, D. Chen, C. Wang, and M. Thatcher, "Constructing weather data for building simulation considering urban heat island," *Building Services Engineering Research & Technology*, vol. 35, no. 1, pp. 69–82, 2014.

[6] S. Oxizidis, A. V. Dudek, and A. M. Papadopoulos, "A computational method to assess the impact of urban climate on buildings using modeled climatic data," *Energy and Buildings*, vol. 40, no. 3, pp. 215–223, 2008.

[7] N. H. Wong, S. K. Jusuf, N. I. Syafii et al., "Evaluation of the impact of the surrounding urban morphology on building energy consumption," *Solar Energy*, vol. 85, no. 1, pp. 57–71, 2011.

[8] N. H. Wong, S. K. Jusuf, A. A. la Win, H. K. Thu, T. S. Negara, and W. Xuchao, "Environmental study of the impact of greenery in an institutional campus in the tropics," *Building and Environment*, vol. 42, no. 8, pp. 2949–2970, 2007.

[9] A. L. S. Chan, "Developing a modified typical meteorological year weather file for Hong Kong taking into account the urban heat island effect," *Building and Environment*, vol. 46, no. 12, pp. 2434–2441, 2011.

[10] D. B. Crawley, L. K. Lawrie, F. C. Winkelmann et al., "EnergyPlus: creating a new-generation building energy simulation program," *Energy and Buildings*, vol. 33, no. 4, pp. 319–331, 2001.

[11] S. E. Belcher, J. N. Hacker, and D. S. Powell, "Constructing design weather data for future climates," *Building Services Engineering Research and Technology*, vol. 26, no. 1, pp. 49–61, 2005.

[12] Central Weather Bureau, *Analysis on the Trend of Global and Taiwan's Climate*, Central Weather Bureau, Taipei, Taiwan, 2010, http://www.cwb.gov.tw/V7/climate/climate_info/monitoring/monitoring_7.html.

[13] Cryopak, *ESCORT iLog User Guide*, Cryopak, New York, NY, USA, 2013, http://www.cryopak.com/en/verification-products/data-loggers/ilog/.

[14] "Thermal environmental conditions for human occupancy," ASHRAE Standard 55, American Society of Heating, Refrigerating and Air Conditioning Engineering, Atlanta, Ga, USA, 2004.

[15] CEN, "Indoor environmental input parameters for design and assessment of energy performance of buildings addressing indoor air quality, thermal environment, lighting and acoustics," CEN Standard EN 15251:2007, CEN, Brussels, Belgium, 2007.

[16] R. L. Hwang, C. P. Chen, F. Y. Lin, W. M. Shih, and K. T. Huang, "Applicability of ASHRAE standard 55 and EN 15251 adaptive thermal comfort models in hot-and-humid climate," in *Proceedings of the Conference of the ISEE, the ISES, and the ISIAQ on Environment and Health*, vol. 55, Basel, Switzerland, August 2013.

[17] F. Nicol and M. Humphreys, "Derivation of the adaptive equations for thermal comfort in free-running buildings in European standard EN15251," *Building and Environment*, vol. 45, no. 1, pp. 11–17, 2010.

[18] International Standards Organization, "Moderate thermal environments—determination of the PMV and PPD indices and specification of the conditions for thermal comfort," ISO 7730:2005, International Standards Organization, Geneva, Switzerland, 2005.